Power System Technology
ISSN:1000-3673

Received: 15-02-2025 Revised: 26-03-2025 Accepted: 18-05-2025

Influence of Temperature on Nickel Oxide Thin Films Fabricated by Spray Pyrolysis using a Solar Oven

Azeddine Rouane[1], Abderrezak Gharbi[2], Aissa Abidi Saad[3]

[1] Laboratory of Dynamics, Interactions and Reactivity Systems DIRS, University of Kasdi Merbah, 30000 Ouargla, Algeria. E-mail : rouane.azeddine@univ-ouargla.dz

[2] Laboratoire de Mécanique Appliquée et Systèmes Energétiques, Université Kasdi Merbah, 30000, Ouargla, Algérie. E-mail : gharbi.abdelrazak@univ-ouargla.dz.

[3] Faculty of Hydrocarbons, Renewable Energies, Earth and Universe Sciences, University of Kasdi Merbah 30000 Ouargla, Algeria. E-mail : abidi.saad@univ-ouargla.dz

Abstract: Nickel oxide (NiO) thin films were deposited on glass substrates using spray pyrolysis to study the effect of fabrication temperature on their structural, optical, and electrical properties. Processing temperatures of 350°C, 450°C, and 550°C were used. X-ray diffraction (XRD) revealed cubic crystals with a single-phase structure oriented along the (220) axis. Grain sizes ranged from 8.2 nm to 64.52 nm. Optical band gaps increased from 3.37 eV to 3.57 eV with higher temperatures, while Urbach energy decreased from 362.12 meV to 280.32 meV. Electrical resistivity varied from 316.22 Ω.cm to 1500.14 Ω.cm, and hole concentration from $5.645x10^{18}$ cm^{-3} to $9.987x10^{18}$ cm^{3}.

Keywords: NiO, X-ray diffraction; Thin Films, Temperature, Solar.

1. Introduction

Nickel nitrate is the inorganic compound Ni (NO3)2 or one of its hydrates. Since the anhydrous form is not common, the term "nickel nitrate" generally refers to nickel (II) nitrate hex-hydrate. The formula for this species is written in two ways: Ni (NO3)2.6H2O and, more descriptively [Ni(H2O)6](NO3)2. This last formula indicates that six water molecules in this hydrated salt surround the nickel (II) center. In the hex-hydrate, the nitrate anions are not bound to the nickel. Three other hydrates are also known: Ni(NO3)2.9H2O, Ni(NO3)2.4H2O and Ni(NO3).2H2O. Anhydrous Ni(NO3)2 is also known [1]. It is prepared by the reaction of nickel oxide with nitric acid. The formation of nickel oxide (NiO) takes place by the thermal decomposition of nickel chloride hexahydrate according to the chemical reaction of equation (Ni(Cl)_2.H_2 O→NiO+2.HCl(g)+5.H_2 O(g)) [2]. Nickel oxide (NiO), belongs to the family of transparent conductive oxides (TCO), it is an antiferromagnetic semiconductor. It is a material recognized by its chemical and thermal stability and presents a set of electrical and optical properties, likely to use in many applications in the field of electronics and optoelectronics [3]. Nickel oxide has a face-centered cubic structure of the NaCl type, with lattice parameter (a = 4.176 Å, It has a volume density of 6.72 g/cm3)) [4, 5]. This structure is composed of two similar sub-lattices A

Power System Technology
ISSN:1000-3673
Received: 15-02-2025 Revised: 26-03-2025 Accepted: 18-05-2025

and B such that any atom of sub-lattice A has only neighbors belonging to sub-lattice B and vice versa. The anion sublattice (O-2) and the cation sublattice (Ni+2) have a CFC structure. Ionic radii: R (Ni+2) = 0.72 Å and R(O-2) = 1.40 Å [6]. This oxide is a transparent material in the visible, whose refractive index is equal to 2.33 with a large direct gap in the ultraviolet range (3.5 - 4 eV) [7]. In addition to the energy level of the 3d electronic subshell responsible for the magnetism was slightly higher than that of the 4S conduction subshell [8]. The order of electrical conductivity in the dark for NiO increases from "10-6 to 10-1" (Ω.cm)-1 with increasing deposition temperature [2, 9].

The variation of the conductivity can correspond with the grain size or with the thickness [9]. It has important physical properties that materials more widely used in various fields and especially in the form of thin layers, especially in the field of electronic optoelectronics and optoelectronics such as (photo-catalytic reactors [10], gas sensors [11], light-emitting diodes [12], optical windows in solar cells [13]. Metal oxide nanostructures with narrow and large band gaps have been widely investigated for their potential applications in various fields [14]. The literature indicates that thin films of NiO, have been produced by several techniques and researchers. These include vacuum evaporation [15], spray pyrolysis [2], sol-gel technique [16], electron beam evaporation [17], sputtering [18], chemical deposition [19], and laser ablation [15]. Most of the reports dealing with the structural aspects of these films [20, emphasize (the effect of the substrate temperature, the electro-chromic property, the cyclic durability, the surface morphology, and the detection property of the films) [21]. The electronic response during potential switching and the degree of coloration [22] as well as their practical use in electrochemical and photovoltaic cells [23].

2. Preparation of cobalt oxide substrates

Nickel oxide thin films (see Fig.1) were synthesized from nickel (II) nitrate hexahydrate Ni (NO3)2,6H2O. Methanol was introduced into the solution to yield a transparent, mildly viscous green solution. Glass substrates were then heated to the required processing temperatures (350°C, 450°C, and 500°C) using a solar oven [24]. According to the work presented by several authors, including Bougrine, A., and al. [25], Chamberlin, R. and, l. [26], the spray pyrolysis method gives a more or less homogeneous product so that it cannot modify the properties from one zone to another. In addition to the substrate's consistency in temperature on the hotplate. The solution is equally dispersed over the substrate's surface because the spraying procedure is perpendicular to the substrate. On hot glass substrates, the resulting solution is pulverized. To achieve the desired thickness, the deposition time is varied between (3 and 4 min), this period is expressed in several time intervals to give the layer sufficient time to crystallize. After setting the glass substrate on the oven's heating plate at the proper temperature for crystallization, we activate the air nebulizer, spray the solution for four minutes, stop for a while to let the substrate

Power System Technology
ISSN:1000-3673
Received: 15-02-2025 Revised: 26-03-2025 Accepted: 18-05-2025

return to its original temperature, and then repeat the procedure until the desired thickness is achieved.

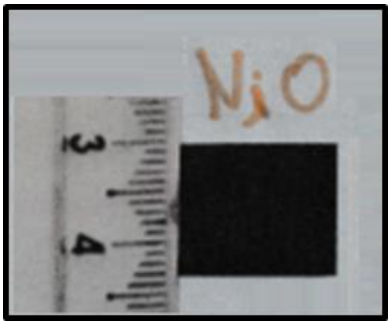

Figure 1. Nickel oxide (NiO) substrate.

3. Structural characterization

Using the Scherrer equation [28, 29], and assuming that the grains are spherical, we can determine the average grain size in the thin film using X-ray diffraction (XRD) spectra through the following equations:

$$D_{(nm)} \frac{0.90.\lambda}{\beta coscos\,\theta} \quad \textbf{(1)}$$

$$\alpha = \frac{4\pi K}{\lambda} \quad \textbf{(2)}$$

Where: (***D***: *Average grain diameter,* ***α***: *Wavelength of incident radiation (1.5 = 1.54056 Å),* ***β*** *: Width at mid-height of the diffraction peak,* ***θ*** *: Diffraction angle and* ***α*** *: Absorption coefficient).*

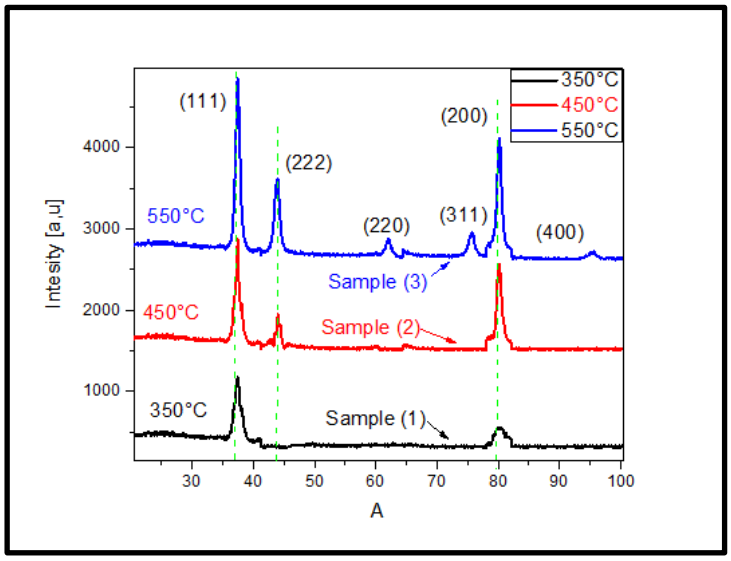

Figure 2. Acoustic parameters of NiO thin films as a function of temperature.

Power System Technology
ISSN:1000-3673
Received: 15-02-2025 Revised: 26-03-2025 Accepted: 18-05-2025

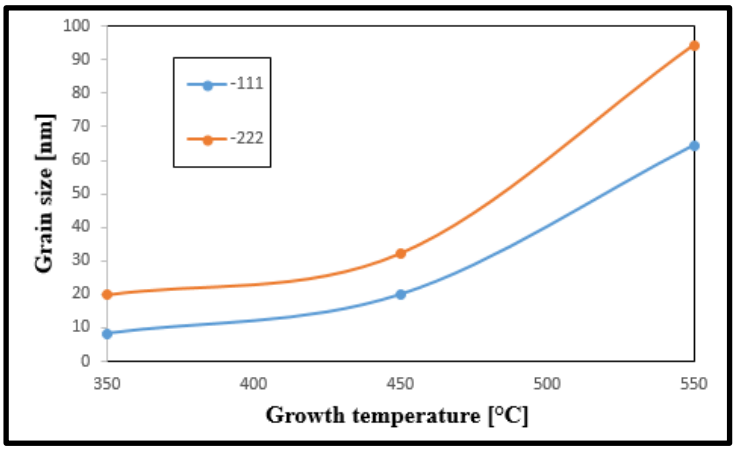

Figure 3. The grain size of the NiO films deposited on sapphire substrates at different temperatures.

With a resolution ranging from a few micrometers to a few tens of nanometers and a very broad depth of focus, SEM allows the generation of surface pictures for all solid materials [29]. This technique scans the sample's surface point by point using a fine beam of electrons. The surface of the sample emits backscattered electrons, secondary electrons, Auger electrons, X-rays, and photons as a result of the interaction of the beam with the material. This interaction takes place in a pear-shaped volume with a size of the order of a cubic micron (m3), making it very large compared to the point of impact [29].

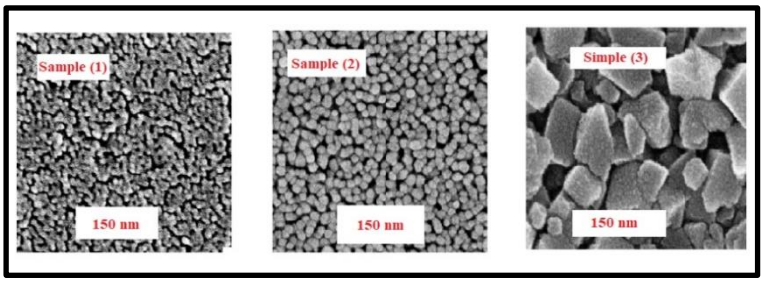

Figure 4. SEM of the NiO films deposited at different temperatures.

4. Optical characterization

The following domains (ultraviolet-visible, infrared, and microwave) can be distingue shed in the fields of spectroscopy according to the wavelength interval in which the measurements are made. In the present work, we used UV-visible spectrophotometry (Cary Series UV-VIS-NIR Spectrophotometer), by which we were able to draw curves representing the variation of the transmittance according to the wavelength in the field of UV-visible and near-infrared (200–800nm). By exploiting these curves, we can determine its optical characteristics; the optical absorption threshold, the absorption coefficient, the valence band tail width, and, the refractive index. The determination of the optical gap (Eg) is based on the model proposed by

Power System Technology
ISSN:1000-3673
Received: 15-02-2025 Revised: 26-03-2025 Accepted: 18-05-2025

Tauc [30, 31], where (Eg) is related to the absorption coefficient. With the use of a UV-Visi-NIR Spectrophotometer) in the present work, we were able to generate curves in the field of UV-visible and near-infrared that show how transmittance varies with the wavelength in the current study (200–800 nm). These curves can be used to calculate the optical properties of the material, including the optical absorption threshold, absorption coefficient, valence band tail width, and refractive index. The model put forth by Tauc [30, 31] is used to determine the optical gap (Eg), where (Eg) is connected to the absorption coefficient by:

$$\sqrt{aE}=A(hv-E_g) \quad (3)$$

Where: (***A:*** *Constant reflecting the degree of disorder of the amorphous solid structure,* ***E****): Expressed in eV, and* ***E=hv:*** *Energy of the photon in eV).*

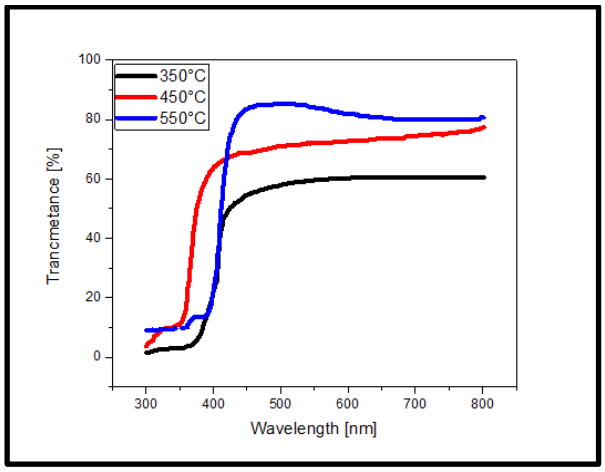

Figure. 5. Transmittance spectra of NiO thin films as a function of processing temperatures.

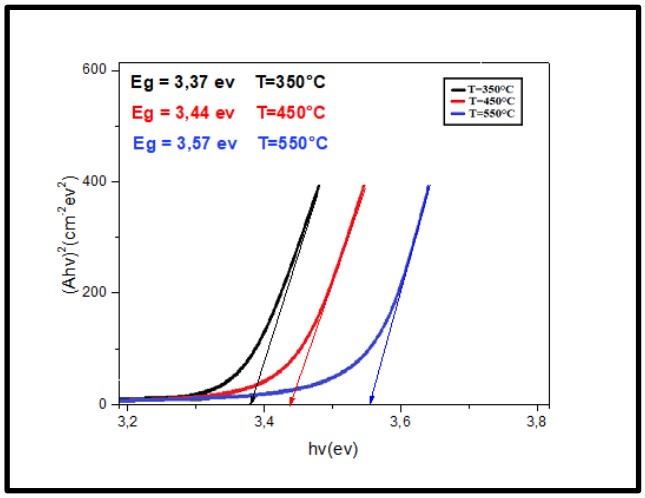

Figure. 6. Optical gaps of NiO thin films.

Power System Technology
ISSN:1000-3673
Received: 15-02-2025 Revised: 26-03-2025 Accepted: 18-05-2025

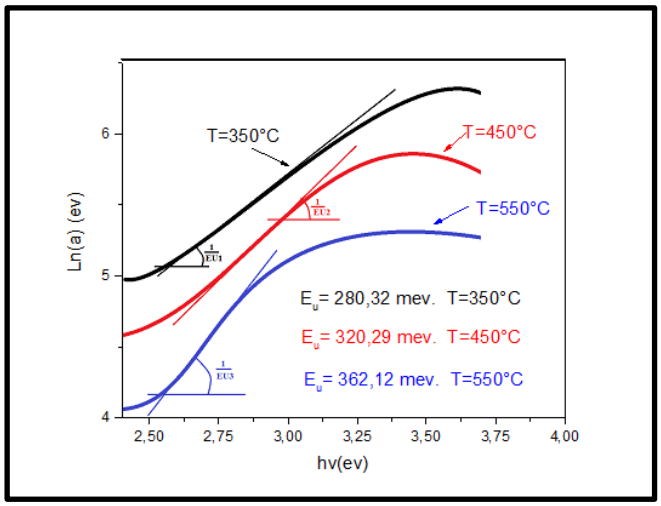

Figure. 7 Urbach parameters (Eu) of NiO thin films.

5. Electrical characterization

To determine the resistivity of our samples, we applied the Hall Effect principle, which relies on two forces: the Lorentz magnetic force and the Hall electrical force acting on a semiconductor carrying a current under a magnetic field. Thus, the Hall Effect is fundamentally grounded in the Lorentz force [32]. We utilized the Ecopia HMS-3000 system, equipped with a magnet generating a magnetic field of 0.55 T, to subject the sample to during electrical measurements, employing a specialized holder. This equipment comprises a comprehensive system capable of measuring resistivity, Hall coefficient, concentration, and mobility. The equipment is a full system for measuring resistivity, Hall coefficient, concentration, and theirity. It uses a sample holder with four tips arranged in a square and is connected to a generator to perform the electrical measurements. The technique involves taking four-point contacts A, B, C, and D, which alternately allow injecting a current Ih (in mA) between two contacts and measuring a voltage Um (in V) between them. By symmetrically placing the contacts and averaging the various measured voltages Um, we can deduce an average resistance Rm (in Ω) that will enable the determination of the resistivity ρ (Ω.cm) of the thin film analyzed with a thickness e (in cm) through the following equation:

$$\rho = \frac{\pi.e.R_m}{ln(2)} \qquad \textbf{(4)}$$

The number of free carriers n (or p) (in cm^-3) is determined by measuring the Hall voltage Uh taken between two contacts as soon as a current IH is applied between the other two under the influence of a magnetic field B of 0.55 Tesla perpendicular to the sample. The orientation of this magnetic field must be adjusted. Additionally, by averaging the different measurements for each of these permutations, we can obtain the value of the average Hall voltage Uhm (in V)

Power System Technology
ISSN:1000-3673
Received: 15-02-2025 Revised: 26-03-2025 Accepted: 18-05-2025

and determine n (or p) as well as the nature of the free carriers (electrons or holes) through the sign associated with the charge q (in C) using the following equation:

$$n(or\ p) = \frac{I_H.B}{\pm q.U_{hm}.e} \quad \textbf{(5)}$$

$$\mu = \frac{1}{|\pm q|.n.p} \quad \textbf{(6)}$$

Table. 1 The Hall measurement result of the samples grown at different temperatures.

Sample	(1)	(2)	(3)
Resistivity (σ[Ω.cm])	316.22	631.45	1500.14
Mobility (μ[cm2 .V-1 .S-1])	0.416	0.677	0.713
Hole Concentration (n[cm-3])	+5.645x10+18	+9.645x10+18	+9.987x10+18
Thickness (e[nm])	340	371	316

6. Results and Discussions

To examine the crystal quality of the NiO films generated at various temperatures, X-ray diffraction measurements of the (2Θ) scan on NiO films were performed. The primary peaks of the [(111) and (222) for the temperature 350°C], [(111), (222) and (200) for the temperature 450°C] and [(111), (222), (200), (220), (3110) and (400) for the temperature450°C] planes connected to NiO films can be seen in Fig. 1, which shows a sizable (111) preferred orientation growth. The very faint peak in Sample (1) is due to the NiO (200) plane's diffraction. Furthermore, it is found that as the growth temperature rises, the structure has more crystallites, which increases the intensity of NiO (111) diffraction [33]. The NiO (111) diffraction peak intensities have a ratio of 1:1.75, 3:25. Additionally, from sample le (1) to sample (3), the full width at half maximum (FWHM) of NiO (111) is decreasing, showing that the NiO film's crystal quality is improved at higher temperatures.

Fig. 3 shows the variations of NiO grain size at different temperatures. The NiO grain size is calculated from the (111) peak using the rider's formula (equation 1). For samples (1), (2), and, (3), the computed findings are 8.2 nm, 19.84, and 64.52 nm, respectively. It suggests that raising the growth temperature might result in larger NiO grains. In addition, the outcome of the SEM pictures, as seen in Fig. 4 supports this. On the one hand, it can be seen from comparing the SEM pictures of the samples above that the NiO films' grain size dramatically increases with rising temperature. While the grain appears to have a cubic shape when the growth temperature reaches 550°C, the grain's shape is aberrant at lower development temperatures. This change is attributed to the NiO film's regular cubical development closely adhering to the NaCl-type structure as the temperature rises and the film's crystal quality improves.

Power System Technology
ISSN:1000-3673
Received: 15-02-2025 Revised: 26-03-2025 Accepted: 18-05-2025

The optical absorption spectra of the aforementioned samples are displayed in Fig. 5 to study how crystal quality affects optical attributes. The optical band gap is calculated from the optical measurements (Equation 3). According to our calculations, the optical band gaps of samples (1), (2), and, (3) are around 3.37 eV, 3.44 eV, and 3.57 eV, respectively. These values are all higher than those of the materials ZnO (3.3 eV) and GaN (3.4 eV). Additionally, it should be noted that when the growth temperature increases, the optical band gap moves toward lower energy. This is most likely related to the improvement in crystallinity and the band tailing brought on by non-stoichiometric composition [34]. The Hall results of the NiO films made at various temperatures are displayed in Table 1 below. All three samples show p-type properties, and the hole concentration decreases with increasing growth temperature. Additionally, as the temperature rises, the films' mobility and resistance increase. It is widely known that NiO materials will display p-type characteristics as an insulator of stoichiometric composition when Ni2 vacancies are present [35]. As a result, the improvement in NiO crystal properties brought on by the higher growing temperature is what causes the increase in hole mobility. AddThe declining Ni2 vacancies should also be blamed for the increased resistivity and decreasing hole concentration [36]. Figure 6 displays the three samples' ultraviolet-visible patterns. Fig. 5 shows how the transmittance rapidly decreases in the low wavelength area close to the absorption edge. The optical absorption spectrum investigation described above shows that the NiO films produced at high temperatures had higher transmittances.

The three NiO samples have respective transmittances of 58%, 69%, and 88% at 425 nm. This shows that the NiO films have good UV-range transmittance properties.

7. Results and Discussions

The findings of the Hall measurement show that all NiO films have p-type conductivity, and their resistance rises as the growth temperature rises. Additionally, the optical transmittance of the NiO films increases from 58% to 88% at 425 nm, with an increase in optical band gap energy values from 3.37 eV to 3.57 eV. This work suggests that NiO films could achieve their maximum conductivity and transmittance at the proper growing temperature films are thought to hold potential for use in the production of UV-LEDs when combined with other n-type large band gap semiconductors.

8. References

[1] K. Lascelles, L. G. Morgan, D. Nicholls, D. Beyersmann, and N. Institute, "Nickel compounds," *Ullmann's Encyclopedia of Industrial Chemistry*, pp. 1-17, 2000.

[2] H. Kamal, E. Elmaghraby, S. Ali, and K. Abdel-Hady, "Characterization of nickel oxide films deposited at different substrate temperatures using spray pyrolysis," *Journal of crystal growth*, vol. 262, no. 1-4, pp. 424-434, 2004.

Power System Technology
ISSN:1000-3673
Received: 15-02-2025 Revised: 26-03-2025 Accepted: 18-05-2025

[3] B. Reguig, M. Regragui, M. Morsli, A. Khelil, M. Addou, and J. Bernede, "Effect of the precursor solution concentration on the NiO thin film properties deposited by spray pyrolysis," *Solar Energy Materials and Solar Cells,* vol. 90, no. 10, pp. 1381-1392, 2006.

[4] J. Wang, P. Yang, X. Wei, and Z. Zhou, "Preparation of NiO two-dimensional grainy films and their high-performance gas sensors for ammonia detection," *Nanoscale research letters,* vol. 10, no. 1, pp. 1-6, 2015.

[5] M. Maache, "Elaborattion de films Minces d'oxydes Semiconducteurs Par Voie sol-Gel," Université Mohamed Khider Biskra, 2014.

[6] S. Le Pévédic, "Etude de la formation et de l'oxydation de couches minces d'alliages Al-Ni après dépôt d'Al sur un monocristal de Ni (111)," 2007.

[7] S. S. Ahmed, E. K. Hassan, and G. H. Mohamed, "Investigation of optical properties of NiO0. 99Cu0. 01 thin film by thermal evaporation," *Int. J,* vol. 2, no. 2, pp. 633-638, 2014.

[8] M. A. Belkhir, "Structure de bandes à spin polarisé par la méthode des fonctions localisées: application à MnO et NiO," Université Paul Verlaine-Metz, 1988.

[9] H. Benzarouk *et al.*, "Effect of different dopant elements (Al, Mg an,d Ni) on microstructural, optical and electrochemical properties of ZnO thin films deposited by spray pyrolysis (SP)," *Superlattices and Microstructures,* vol. 52, no. 3, pp. 594-604, 2012.

[10] B. Lin, Z. Fu, and Y. Jia, "Green luminescent center in undoped zinc oxide films deposited on silicon substrates," *Applied physics letters,* vol. 79, no. 7, pp. 943-945, 2001.

[11] A. Sekar, S. Kim, A. Umar, and Y. Hahn, "Catalyst-free synthesis of ZnO nanowires on Si by oxidation of Zn powders," *Journal of Crystal Growth,* vol. 277, no. 1-4, pp. 471-478, 2005.

[12] A. Umar, S. Lee, Y. Lee, K. Nahm, and Y. Hahn, "Star-shaped ZnO nanostructures on silicon by cyclic feeding chemical vapor deposition," *Journal of Crystal Growth,* vol. 277, no. 1-4, pp. 479-484, 2005.

[13] S. Studenikin, N. Golego, and M. Cocivera, "Optical and electrical properties of undoped ZnO films grown by spray pyrolysis of zinc nitrate solution," *Journal of Applied Physics,* vol. 83, no. 4, pp. 2104-2111, 1998.

[14] K. Ukoba, A. Eloka-Eboka, and F. Inambao, "Review of nanostructured NiO thin film deposition using the spray pyrolysis technique," *Renewable and Sustainable Energy Reviews,* vol. 82, pp. 2900-2915, 2018.

Power System Technology
ISSN:1000-3673
Received: 15-02-2025 Revised: 26-03-2025 Accepted: 18-05-2025

[15] B. Sasi and K. Gopchandran, "Preparation and characterization of nanostructured NiO thin films by reactive-pulsed laser ablation technique," *Solar Energy Materials and Solar Cells*, vol. 91, no. 15-16, pp. 1505-1509, 2007.

[16] S. Heusing and M. Aegerter, "Sol-gel coatings for electrochromic devices," in *Sol-gel processing for conventional and alternative energy*: Springer, 2012, pp. 239-274.

[17] T. Seike and J. Nagai, "Electrochromism of 3d transition metal oxides," *Solar energy materials*, vol. 22, no. 2-3, pp. 107-117, 1991.

[18] K. Yoshimura, T. Miki, and S. T. S. Tanemura, "Nickel oxide electrochromic thin films prepared by reactive DC magnetron sputtering," *Japanese journal of applied physics*, vol. 34, no. 5R, p. 2440, 1995.

[19] A. Varkey and A. Fort, "Solution growth technique for deposition of nickel oxide thin films," *Thin Solid Films*, vol. 235, no. 1-2, pp. 47-50, 1993.

[20] K. D. Lee and W. C. Jung, "Effect of substrate temperature on the electrochromic properties and cyclic durability of nickel oxide films," *Journal of the Korean Physical Society*, vol. 45, no. 2, pp. 447-454, 2004.

[21] D.-m. Na, L. Satyanarayana, G.-P. Choi, Y.-J. Shin, and J. S. Park, "Surface morphology and sensing property of NiO-WO3 thin films prepared by thermal evaporation," *Sensors*, vol. 5, no. 12, pp. 519-528, 2005.

[22] E. Avendaño, L. Berggren, G. A. Niklasson, C. G. Granqvist, and A. Azens, "Electrochromic materials and devices: Brief survey and new data on optical absorption in tungsten oxide and nickel oxide films," *Thin solid films*, vol. 496, no. 1, pp. 30-36, 2006.

[23] M. D. Irwin, D. B. Buchholz, A. W. Hains, R. P. Chang, and T. J. Marks, "p-Type semiconducting nickel oxide as an efficiency-enhancing anode interfacial layer in polymer bulk-heterojunction solar cells," *Proceedings of the National Academy of Sciences*, vol. 105, no. 8, pp. 2783-2787, 2008.

[24] A. Gharbi, S. Benramache, L. Fellah, and A. Zedouri, "Investigation of the Temperature on the Thin Layers of Cobalt Oxide Produced by the Spray Pyrolysis Method Using a Solar Oven," *Annals of the West University of Timisoara. Physics Series*, vol. 63, pp. 163-176, 2021.

[25] A. Bougrine, A. El Hichou, M. Addou, J. Ebothé, A. Kachouane, and M. Troyon, "Structural, optical and cathodoluminescence characteristics of undoped and tin-doped ZnO thin films prepared by spray pyrolysis," *Materials Chemistry and Physics*, vol. 80, no. 2, pp. 438-445, 2003.

Power System Technology
ISSN:1000-3673
Received: 15-02-2025 Revised: 26-03-2025 Accepted: 18-05-2025

[26] R. Chamberlin and J. Skarman, "Chemical spray deposition process for inorganic films," *Journal of the Electrochemical Society*, vol. 113, no. 1, p. 86, 1966.

[27] M. Ohring, "Characterization of Thin Films and Surfaces," *Materials Science of Thin Films*, pp. 559-640, 2002.

[28] B. Cullity, "Elements of X-ray Diffraction. Addison and Wesley Publishing Company Inc," *Reading, USA*, pp. 32-106, 1978.

[29] A. Douayar, "Contribution à l'étude des propriétés structurales, optiques et électriques des couches minces de l'oxyde de zinc (ZnO) dopé (fluor, indium, aluminium et néodyme)," 2013.

[30] L. Miao, P. Jin, K. Kaneko, A. Terai, N. Nabatova-Gabain, and S. Tanemura, "Preparation and characterization of polycrystalline anatase and rutile TiO2 thin films by rf magnetron sputtering," *Applied Surface Science*, vol. 212, pp. 255-263, 2003.

[31] M. Abdel-Aziz, I. Yahia, L. Wahab, M. Fadel, and M. Afifi, "Determination and analysis of dispersive optical constant of TiO2 and Ti2O3 thin films," *Applied surface science*, vol. 252, no. 23, pp. 8163-8170, 2006.

[32] E. H. Putley, *The Hall effect,t, and related phenomena*. Butterworths, 1960.

[33] A. Ashour, N. El-Kadry, and S. Mahmoud, "On the electrical and optical properties of CdS films thermally deposited by a modified source," *Thin solid films*, vol. 269, no. 1-2, pp. 117-120, 1995.

[34] T. Dutta, P. Gupta, A. Gupta, and J. Narayan, "Effect of Li doping in NiO thin films on its transparent and conducting properties and its application in heteroepitaxial pn junctions," *Journal of Applied Physics*, vol. 108, no. 8, p. 083715, 2010.

[35] Z. Jarzebski and J. Marton, "Physical properties of SnO2 materials: I. preparation and defect structure," *Journal of the electrochemical Society*, vol. 123, no. 7, p. 199C, 1976.

[36] S.-C. Chen, T.-Y. Kuo, and T. Sun, "Microstructures, electrical and optical properties of non-stoichiometric p-type nickel oxide films by radio frequency reactive sputtering," *Surface and Coatings Technology*, vol. 205, pp. S236-S240, 2010.